

The Possible Curative Role of Bone Marrow-Derived Mesenchymal Stem Cells in Bleomycin-Induced Skin Changes in Adult Male Albino Rats

Original
Article

Amal Ali Abd-Elhafez, Maram Mohamed Elkelany, Amany Mohamed Ibrahim Mousa, Thoraya Abd El-Aziz Ali El-deeb and Amira Adly Kassab

Department of Histology, Faculty of Medicine, Tanta University, Egypt

ABSTRACT

Introduction: Bleomycin is a chemotherapeutic agent that has been applied in the treatment of many tumors. Its application results in various cutaneous side effects. The role of bone marrow-derived mesenchymal stem cells [BM-MSCs] has been proved in tissue regeneration.

Aim of the Work: Study of the effect of bleomycin on the histological structure of the skin of adult male albino rats and evaluation of the possible curative role of BM-MSCs.

Materials and Methods: Forty-five adult male albino rats were divided into two groups. Control group included 15 rats. Experimental group included 30 rats which were subdivided into three equal subgroups: 2A, 2B & 2C. Rats of the experimental group were injected with bleomycin subcutaneously for four weeks. Each rat of subgroup 2A received [0.1mg] of bleomycin. Each rat of subgroup 2B received [1ml] of the culture media of the bone marrow cells one day after the last bleomycin dose. Each rat of subgroup 2C received BM-MSCs (2.5×10^6) one day after the last bleomycin dose. Skin specimens were examined by the light and electron microscopy. Immunohistochemical study was done by using antibodies to transforming growth factor beta (TGF- β). Evaluation of the collagen surface area percentage and the number of TGF- β positive cells was performed.

Results: Experimental subgroups 2A & 2B showed the disturbance of the normal architecture of the skin. There was a significant increase in the surface area percentage of collagen and number of TGF- β positive cells. Ultrastructurally, some keratinocytes showed cytoplasmic vacuolation, swollen disrupted mitochondria and nuclear changes. In contrast, the experimental subgroup 2C showed minimal structural changes and a non-significant difference in all mentioned parameters.

Conclusion: Bleomycin altered the normal structure of the skin of adult male albino rats. Bone marrow-derived MSC improved the skin changes induced by bleomycin.

Received: 15 June 2021, **Accepted:** 19 August 2021

Key Words: Bleomycin, BM-MSCs, electron microscopy, immunohistochemistry, skin.

Corresponding Author: Amira Adly Kassab, MD, Department of Histology, Faculty of Medicine, Tanta University, Egypt, **Tel.:** +20 10 1669 7635 **E-mail:** amirakassab80@yahoo.com

ISSN: 1110-0559, Vol. 45, No. 4

INTRODUCTION

Bleomycin is an antibiotic as well as an antitumor agent. It has been used for treatment of many cancers. Despite the appearance of new agents in oncology, bleomycin remains necessary in many chemotherapy regimens for Hodgkin's lymphoma and germinative tumors. On the other hand, bleomycin has many complications of lung and skin^[1].

Skin reactions are the most common side effects that include erythema, hyperpigmentation of the skin, striae, vesiculation and ulceration. These manifestations usually occur when the cumulative dose of bleomycin has reached more than 100U^[2]. A mouse model of bleomycin-induced dermal fibrosis has induced which mimics early and inflammatory stages of human systemic scleroderma. Scleroderma is an autoimmune connective tissue disorder that affects mainly the skin^[3].

Bleomycin has been associated with temporary hair loss and nail pigmentation. The pigment is deposited in horizontal or vertical bands, which may be brown or blue, and generally grow out with the nail^[4].

Nowadays, bone marrow-derived mesenchymal stem cells (BM-MSCs) play an important role in tissue repair or regeneration. They are characterized by their easy isolation and culture. BM-MSCs have a role in improving tissue fibrosis due to various diseases such as stroke and myocardial infarction^[5]. These cells also have a therapeutic role in cases of liver fibrosis^[6]. Moreover, they are applied as an efficient therapy for many skin disorders as psoriasis, skin burn and alopecia^[7,8].

So, this scientific work was performed to study the effect of bleomycin on the histological structure of the skin of adult male albino rats and to evaluate the possible curative role of BM-MSCs by some histological techniques.

MATERIALS AND METHODS

Chemicals

- Bleomycin: bleomycin ampule [15 mg] was purchased from Nippon Kayaku Co.[Ltd., Tokyo, Japan], Catalogue number 971,CAS number 9041-93-4.

- Roswell Park Memorial Institute (RPMI) 1640 medium: 1640 with L- glutamine, liquid, sterile-filtered was purchased in sterile bottle (500 ml) from Lonza Company, cat. No. BE12-702F, Swiss. It was stored at 4 °C.
- Fetal bovine serum (FBS) was a product of Gibco, Invitrogen Co., Cat. No A11-151, Austria. It was stored at – 20 °C.
- Antibiotic-Antimycotic: (Penicillin-Streptomycin-Amphotericin-B Mixture) was purchased from Lonza CO., Cat. No: 17-745 E, Switzerland. It contained penicillin (10,000 units/ml penicillin G sodium) and streptomycin (10,000µg/ml streptomycin in sulphate) and was stored at –20 °C.
- Phosphate Buffered Saline (PBS) (0.0067 M (PO₄) without Ca and Mg) was purchased from Lonza Bioproduct, cat. No: BE 17-512 F, Switzerland. It included 8 gm NaCl, 0.25 gm KCl, 144 gm Na₂HPO₄ and 0.25 gm KH₂PO₄, PH 7.4. It was stored at 4 °C.
- Trypsin/EDTA solution was purchased from Lonza Co., Cat. No: BE 17-161E, Switzerland. It is Trypsin-EDTA 200 mg/l versene (EDTA) 170.000U Trypsin/L sterile filtered for cell culture. It was stored at – 20 °C.

Animal grouping

The experiment was done in the Tissue Culture Unit of Histology Department, Faculty of Medicine according to the Ethical Committee recommendations of Tanta University [Approval Code:30966/05/16].

Forty-five adult male albino rats aging 10-12 weeks and weighing 200-250 grams were used in this study. The rats were obtained from the animal house of Tanta Faculty of Medicine. They were housed in clean, suitable, properly ventilated plastic cages under controlled conditions of temperature, humidity and a 12-h light/dark cycle and were fed on a similar commercial laboratory diet and water. The rats were acclimatized to their environment at least one week before the experiment. They were divided into two groups:

1-Control group: It included 15 rats and was subdivided into:

- Subgroup 1A: It included 5 rats. Skin specimens were taken from their shaved mid back. The bone marrow of their femurs, tibias and humeri were extracted and cultured for mesenchymal stem cells (MSCs).
- Subgroup 1B: It included 5 rats that were subcutaneously injected with 0.1ml saline [vehicle for bleomycin] in the shaved mid back daily for 4 weeks. Skin specimens were taken from their shaved mid back after 4 weeks from the last day of saline injection.

- Subgroup 1C: It included 5 rats. They were once subcutaneously injected in the shaved mid back with 1ml of the freshly prepared culture media [45 ml of RPMI, 5 ml of FBS and 0.5 ml Antibiotic/antimycotic mix] that was used for bone marrow cells. Skin specimens were taken from their mid back after 4 weeks of media injection.

2-Experimental group: It included 30 rats and was subdivided into:

- Subgroup 2A (Bleomycin group): Ten rats were daily injected with bleomycin [0.1 mg dissolved in 0.1 ml saline] subcutaneously in the shaved mid back for 4 weeks. Skin specimens were taken from their mid back after 4 weeks from the last day of bleomycin injection^[9].
- Subgroup 2B (Bleomycin and Culture media group): Ten rats were subcutaneously injected with bleomycin in the shaved mid back at the same dose and duration as subgroup 2A and one day after the last bleomycin injection, each rat received subcutaneously 1ml of the freshly prepared culture media. Skin specimens were taken from their mid back after 4 weeks of media injection.
- Subgroup 2C (Bleomycin and BM-MSCs group): Ten rats were subcutaneously injected with bleomycin in the shaved mid back at the same dose and duration as subgroup 2A and one day after the last bleomycin injection, each rat received BM-MSCs [2.5×10⁶ in 1ml media] subcutaneously in the mid back. Skin specimens were taken from their mid back after 4 weeks of MSCs injection^[10].

At the appropriate time [4 weeks from the last injection in each subgroup], the animals were anesthetized by intraperitoneal injection of sodium pentobarbital [50 mg/Kg]^[11] and the skin specimens were processed for histological examination.

Collection, culture of BM-MSCs and preparation of MSCs suspension:

The five rats of subgroup 1A were used as a source for BM-MSCs. The bone marrow of the femurs, tibias and humeri of rats were extracted, collected and cultured for mesenchymal stem cells (MSCs). It was called passage 0 (P0) in the 1st day. When MSCs (P0) reached confluence (70- 80%) after about (7-9) days, subculture was done to reach passage 1 (P1) which upon reaching confluence (70-80%), trypsinization was done to reach passage 2 (P2) which upon reaching confluence (70-80%) trypsinization was done to reach passage 3 (P3).

A. Bone marrow harvesting

The rats were sacrificed and were sunken in 70% alcohol before dissection for sterilization of the skin surface. The femurs, tibias and humeri were carefully dissected from adherent soft tissues. Then they were placed into sterilized petri dishes containing the culture media and antibiotic for

1-2 minutes, and then transferred to the cell culture lab for isolation of the bone marrow. The isolation process was carried out in a laminar flow cabinet. Epiphyses of both ends of the bones were cut away from the diaphysis using a sterilized bone cutting scissor. The bone marrow was flushed out from the diaphysis of the bones by inserting a syringe needle filled with 3 ml of the freshly prepared culture media into one end of the bones. The marrow plugs were expelled from the opposite end of bones into tissue culture flask (25 ml) and was completed to 7 ml with the culture media to cover the surface of culture flask (0.4 ml media/1 cm² surface area). The flasks were labeled (cells name, passage number and date). Culture flasks were kept at 37°C in 5% CO₂ incubator^[12].

B. Culture and expansion of MSCs

The cultured cells were examined daily by using the inverted microscope to assess the level of expansion of the cultured MSCs and to detect the appearance of any bacterial or fungal infection. Three days after primary culture, the non-adherent cells were removed by aspiration, using a sterile pipette. The adherent cells were then washed twice with Phosphate Buffered Saline (PBS). Then, 7 ml of the fresh culture media was added to each flask. MSCs were distinguished from other BM cells by their tendency to adhere to the tissue culture plastic flask. The culture medium was replaced every 2 days, so the non-adherent cells were aspirated and discarded, using a sterile pipette. The cells were washed with PBS before adding the fresh medium, so the second exchange of medium was done after 5 days when spindle shaped cells appeared with long processes and vesicular nuclei^[13].

C. Trypsinization of BM- MSCs

Trypsinization is used to dislodge cells from the flask. The culture media in the flasks were aspirated by sterile plastic pipette and the cultured cells were washed with PBS. The PBS was removed and about 2.5 ml of trypsin / EDTA solution (used at a working concentration of 0.25%) was shortly pre-warmed to 37°C and was then added to the cells to detach them from the floor of the flask. The flasks containing trypsin / EDTA solution were incubated at 37°C for about 2 minutes. Then, the flasks were checked under inverted microscope to make sure that adherent cells were separated from the floor of the flask. The detached cells appeared rounded and floating. The action of trypsin/EDTA was stopped by adding 7.5 ml of complete medium then the cell suspension was aspirated using pipette and was put in Falcon culture tube (15ml). The cells were centrifuged at 800 RPM for 5 minutes in the centrifuge. The supernatant was discarded and the cell pellets were re-suspended into fresh complete medium. Then, cell counting and viability was performed using a hemocytometer to determine the total cell count^[14].

D. Counting of the MSCs

The hemocytometer was used to determine the total cell count and to assess viability of the cells. The

hemocytometer slide consists of two chambers, each of which is divided into nine squares with a dimension of 1x1 mm. A cover glass is supported over these squares, so in total each large square has volume of 0.0001 ml. Trypan blue 0.4% is used for viable cell counting. Living cells do not take up certain dyes, whereas dead cells do. A cell suspension (5 ml) was prepared from diluted suspension after trypsinization. Then, 0.5ml of cell suspension was mixed with 0.5ml of trypan blue suspension (0.4%). This 1:1 dilution of the cells and dye was allowed to stand for about 2 minutes then shaken well. A pipette tip was used to transfer a small amount of trypan blue cell suspension to both chambers of the hemocytometer by carefully touching the edge of the cover slip with the pipette tip and allowing each chamber to fill up by capillarity property. All cells in the four 1 mm corner square were counted. In addition, the viable and non-viable cells were counted separately^[15]. The cell concentration was calculated as follows:

Cells/ml = mean cell count per square x dilution factor (1) x 10⁴^[16].

E. Preparation of MSC suspension

The cells of passage 3 (P3) are ready for injection. The cell suspension was transferred to a sterile culture tube. The sterile tube was exposed to centrifugation at 2000 rpm for 10min. The supernatant was removed carefully by gentle aspiration using a sterile pipette so as not to disturb the cell pellet (Sun *et al.*, 2003). The cell suspension in the sterile tube was prepared to perform cell viability by trypan blue and cell count using a hemocytometer. The total viable cells injected were 2.5×10⁶ / rat^[10].

For light microscopy

The specimens were fixed in 10% neutral-buffered formalin for 24 hours, washed, dehydrated, cleared and paraffin immersed. Then, sections were cut (5µm thickness) and stained with hematoxylin and eosin [H&E] and Mallory's trichrome stains^[17].

For electron microscopy

The specimens were rapidly fixed in 2.5% phosphate buffered glutaraldehyde. The sample processing was done according to routine protocols. Semithin sections were prepared and stained with toluidine blue (1%) to select areas needed for ultrastructural examination. Sections of 75 nm in thickness were cut and were picked upon 200 mesh uncoated copper grids. Then, the grids were double stained, with uranyl acetate and lead citrate^[18]. Finally, the specimens were examined and photographed using (JEOL-JEM-100 SX electron microscope, Japan) with AMT camera at The Electron Microscopic Unit, Tanta Faculty of Medicine and (JEOL-JEM-2100 electron microscope) with Gatan microscopy suite camera at the Electron Microscopic Unit, Faculty of Agriculture, Mansoura University.

Immunohistochemistry for detection of transforming growth factor beta (TGF-β)

Skin sections [5µm thickness] were deparaffinized, rehydrated, and rinsed in phosphate buffered saline. Then,

the sections were incubated in a moist chamber with the primary antibody [Monoclonal rabbit antibody to TGF- β at adilution of 1:80 (clone MCA 797, AbD Serotec, Oxyford, UK)] in phosphate buffered saline overnight at 4 °C. Thereafter, it was rinsed in the same buffer, and co-incubated for an hour with biotinylated secondary antibody {Dako North America, Inc., CA, USA} at the room temperature. Streptavidin peroxidase was added for ten minutes and washed three times in the phosphate buffered saline. The immunoreactivity was visualized using 3, 3'-diaminobenzidine [DAB]-hydrogen peroxide {a chromogen}. Finally, all slides were counterstained using Mayer's haematoxylin. The negative control slides were processed without usage of the primary antibody^[19,20]. A positive control section of prostate was provided by lab Vision Thermo Company.

Morphometric study and statistical analysis

A Leica microscope (DM3000; Leica Microsystems, Wetzlar, Germany) coupled to a CCD camera (DFC-290; Leica, Heerbrugg, Switzerland) was used to obtain the images. Image evaluation was performed using an image analysis computer system (Leica Q 500 MC program) at Central Research Lab., Tanta Faculty of Medicine, Tanta University. Surface area percentage (%) of collagen was measured in 10 non-overlapping fields of each slide at a magnification of X 200^[21]. Moreover, the number of TGF- β positive cells was calculated in 10 non-overlapping fields of each slide at a magnification of X 400^[22].

The area percentage (%) of collagen and the number of TGF- β positive cells were subjected to one-way analysis of variance {ANOVA} as well as Tukey's procedure. Statistical package for social sciences statistical analysis software {SPSS Inc., version 11.5, USA} was utilized. The mean values as well as the standard deviation values [Mean \pm SD] for all subgroups were obtained. Probability values {*P values*} < 0.05 and < 0.001 were significant and highly significant values respectively.

RESULTS

All rats tolerated all experimental procedures and survived until the end of the experiment.

Morphological identification of BM-MSCs using inverted microscope

BM-MSCs were spindle or star shaped (Figure 1A). The cells showed multiple interdigitating processes with central vesicular nuclei and multiple nucleoli (Figures 1A,B). BM-MSCs showed confluence at different stages (50% and 80%) (Figures 1B,C). After trypsinization, the cells appeared rounded and crowded in colonies (Figure 1D).

Light microscopic results

I-Haematoxylin and Eosin

1-Control group

Skin sections of all control subgroups revealed the same normal histological structure. The epidermis

was keratinized stratified squamous epithelium (Figures 2A,2B) that was mainly formed of arranged keratinocytes in four layers. The stratum basale rested on a basement membrane and was formed of low columnar cells with basal oval nuclei. The stratum spinosum consisted of polyhedral cells with central rounded nuclei. The stratum granulosum showed spindle-shaped cells with dark granules. Finally, the superficial non-cellular horny layer of keratin was the acidophilic stratum corneum (Figure 2C). The border between the epidermis and dermis was demarcated (prominent dermo-epidermal junction). The underlying papillary layer of the dermis showed blood capillaries and connective tissue cells, whereas the inner reticular layer of the dermis was composed of a dense connective tissue rich in fibers. The dermis contained hair follicles with sebaceous glands (Figures 2A,2B).

2- Experimental group

a- Subgroup 2A (Bleomycin group)

Skin specimens of bleomycin-treated animals showed disturbance of the normal architecture of the skin with different degrees of severity from an area to another. Loss of definite demarcation between epidermis and dermis, lost epidermal strata arrangement, absent keratin and surface erosion were found (Figure 3A). The absent basement membrane of the epidermis and appearance of spaces between epidermal cells were observed (Figure 3B). Moreover, a homogenous acidophilic material was noticed in the reticular dermis. Sebaceous glands showed proliferation of its cells (Figure 3C).

b- Subgroup 2B ((Bleomycin and Culture media group)

Skin specimens of bleomycin and Culture media-treated animals showed marked disorganization of the epidermal layers with separation of some basal cells of the epidermis and appearance of some epidermal cells with vacuolated cytoplasm and small dark nuclei. The dermis showed some engorged blood vessels and mononuclear cellular infiltration (Figures 4A,4B).

c- Subgroup 2C (Bleomycin and BM-MSCs group)

Skin specimens of bleomycin and BM-MSCs-treated animals revealed minimal structural changes. The epidermis showed more or less normal arrangement of its four strata. Occasionally, some epidermal cells appeared with vacuolated cytoplasm and small dark nuclei. The dermis showed more or less normal arrangement of its fibers (Figure 4C).

II-Mallory's trichrome stain

1-Control group

All subgroups showed normal appearance and arrangement of collagen fibers [blue in color] in both the papillary and reticular layers of the dermis. The papillary layer showed small aggregates of collagen fibers which appeared as a fine loosely arranged network. Deep in

the reticular layer, collagen became more abundant and appeared as thick irregular bundles (Figure 5A).

2- Experimental group

a- Subgroup 2A (Bleomycin group)

Skin specimens showed an apparent increase in the thickness of collagen bundles in both the papillary and reticular dermis with subsequent decrease in the amorphous matrix between them (Figure 5B).

b- Subgroup 2B ((Bleomycin and Culture media group)

Skin specimens also showed an apparent increase in the thickness of collagen bundles in both the papillary and reticular dermis with subsequent decrease in the amorphous matrix between collagen fibers (Figure 5C).

c- Subgroup 2C (Bleomycin and BM-MSCs group)

Skin specimens showed partial improvement in many areas. A few areas in the papillary dermis showed apparent thick collagen bundles, while the reticular dermis showed more or less normal arrangement of collagen bundles (Figure 5D).

III-Immunohistochemistry (TGF- β)

The negative control sections showed negative TGF- β immunoreaction (Figure 6A).

1-Control group

All subgroups showed a few cells with positive brown cytoplasmic immuno-reaction in the reticular dermis. This reaction was also observed in the cytoplasm of cells of hair follicles and sebaceous glands (Figure 6B).

2- Experimental group

a- Subgroup 2A (Bleomycin group)

Skin specimens showed numerous cells with positive immuno-reaction (nuclear and cytoplasmic) in the reticular dermis (Figure 6C).

b- Subgroup 2B ((Bleomycin and Culture media group)

Skin specimens showed numerous cells with positive immuno-reaction (nuclear and cytoplasmic) in the reticular dermis (Figure 6D).

c- Subgroup 2C (Bleomycin and BM-MSCs group)

Skin samples showed a few cells with positive immuno-reaction in the reticular dermis (Figure 6E).

Electron microscopic results

I-Control group

Ultrathin sections of all control subgroups showed the same ultrastructure of the epidermis. Stratum basale

contained oval to rounded nuclei. The basal aspects of keratinocytes were attached to the basement membrane with hemidesmosomes (Figure 7A). Next to the stratum basale, the stratum spinosum was observed containing tonofilaments as well as oval to rounded nuclei with prominent nucleoli and extended chromatin. The next layer was stratum granulosum which showed cells with oval to rounded keratohyalin granules in their cytoplasm. The most superficial layer was stratum corneum showed flattened non-nucleated cells whose cytoplasm was filled with regularly arranged keratin (Figure 7B).

II- Experimental group

Subgroup 2A

Ultrathin sections showed different ultrastructural changes. Some keratinocytes showed cytoplasmic vacuolation and swollen mitochondria with disrupted cristae. Moreover, nuclear changes were observed in some keratinocytes such as irregular dark nuclei with condensed heterochromatin and dilatation of perinuclear space (Figures 8A,8B).

Subgroup 2B

Ultrathin sections showed focal widening of the intercellular spaces. Some cells of stratum basale showed abnormal transversely oriented nuclei (Figure 9A). Stratum granulosum showed large sized keratohyalin granules, cytoplasmic vacuolation and irregular nuclei (Figure 9B).

Subgroup 2C

Ultrathin sections showed mild ultrastructural changes. Most cells of stratum basale appeared more or less normal with euchromatic oval nuclei and normal basement membrane (Figure 10A). Cells of stratum spinosum showed a few cytoplasmic vacuoles and normal nuclei with prominent nucleoli (Figure 10B).

Morphometric study & Statistical analysis

1-Surface area % of collagen (Histogram I)

Surface area % of collagen of subgroup 2A and subgroup 2B showed an extremely significant increase when compared with the control group. However, surface area % of collagen of subgroup 2C showed a non-significant difference when compared with the control group.

2- Count of TGF- β positive cells (Histogram II)

The count of TGF- β positive cells in subgroup 2A and subgroup 2B showed an extremely significant increase when compared with the control group. However, subgroup 2C showed a non-significant difference when compared with the control group.

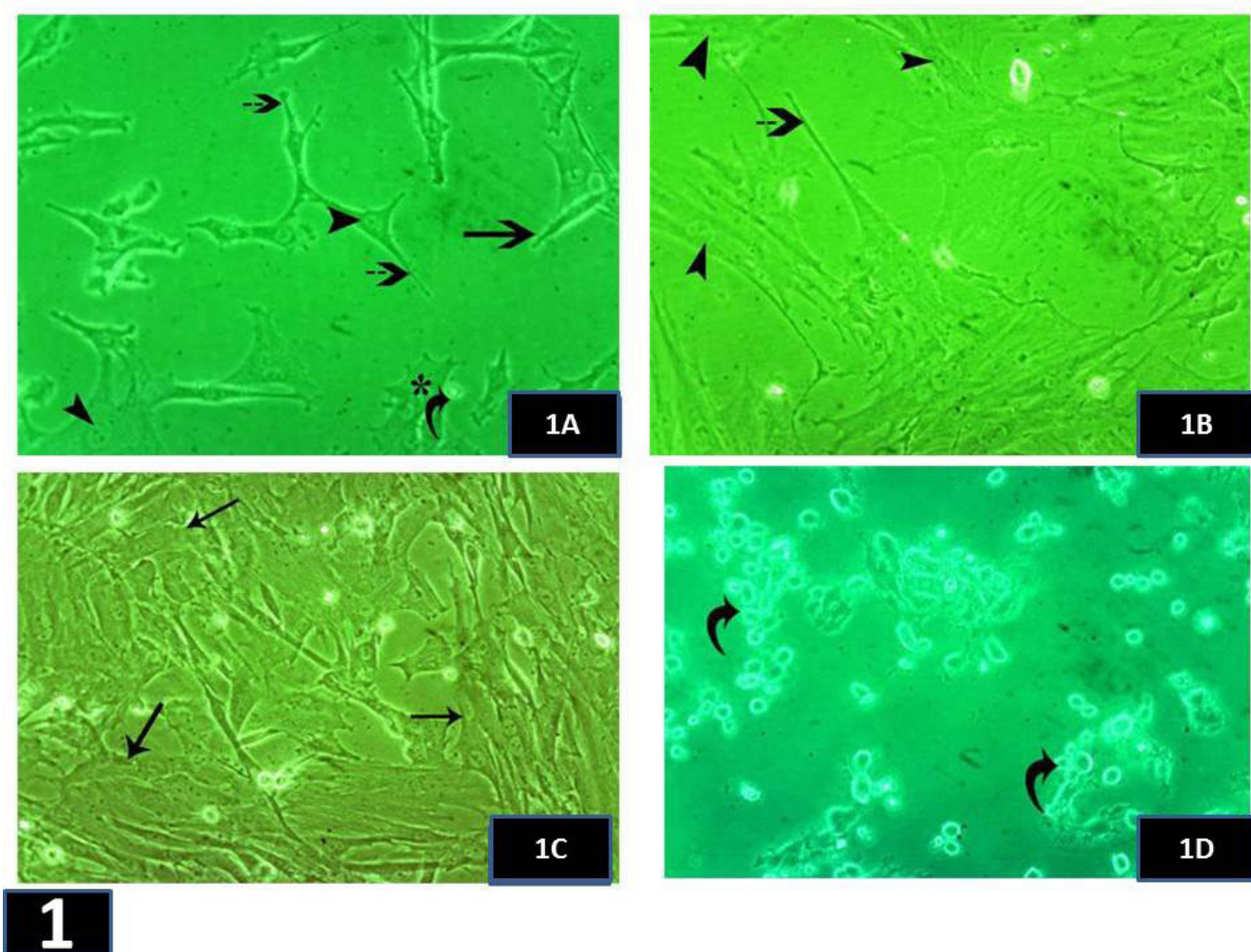


Fig. 1: Photomicrographs of BM-MSCs (1A&1B) show spindle-shaped (→) and star-shaped (*) BM-MSCs with many processes (→→) and rounded vesicular nuclei (▶). The non-adherent cells appear rounded (curved arrow) in (1A). (1B) shows the cultured cells that reach around 50% confluence while (1C) shows cultured cells that reach around 80% confluence (→). (1D) shows rounded and crowded BM-MSCs after trypsinization (curved arrows). (Inverted Microscope, × 400)

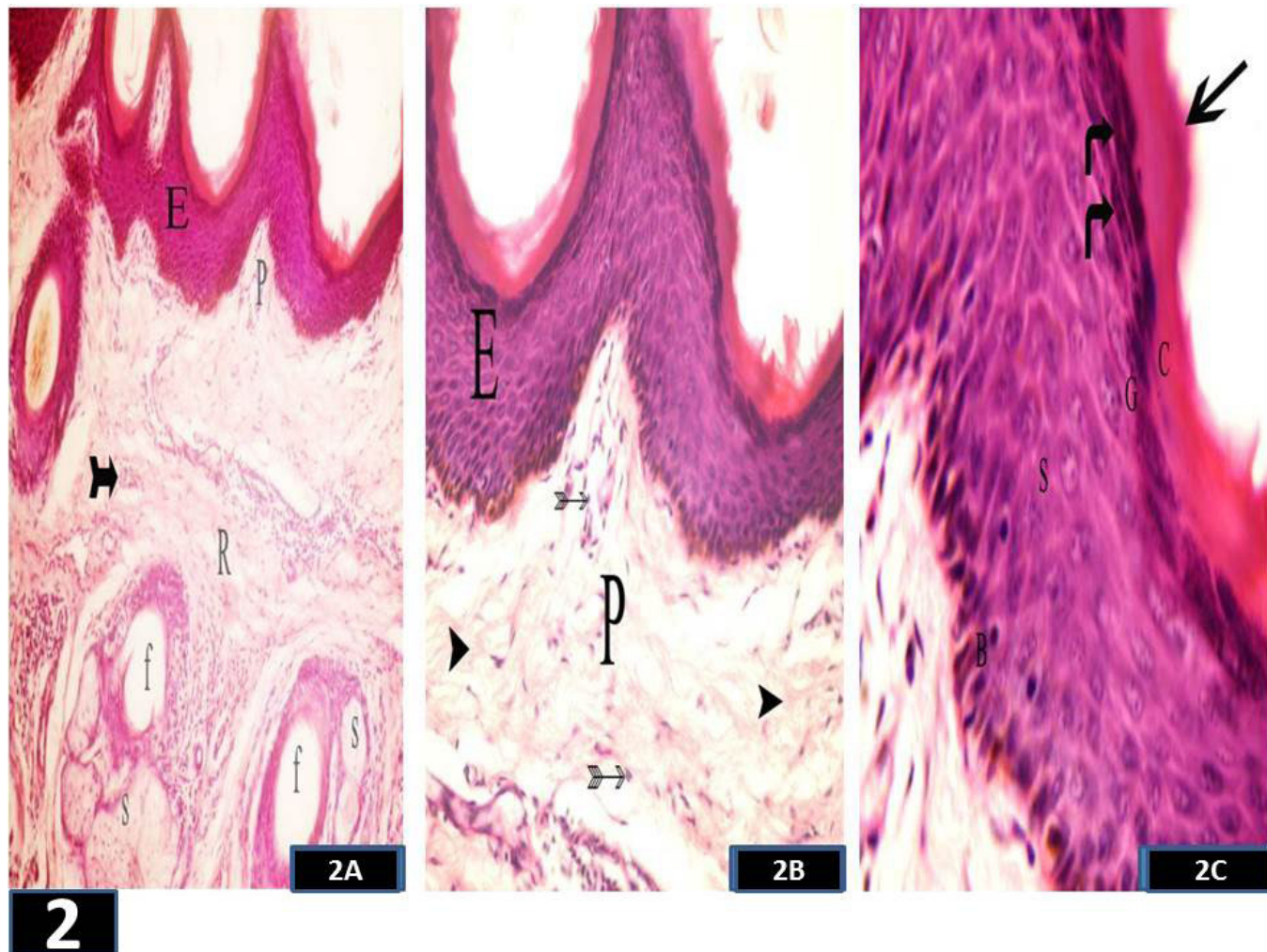


Fig. 2: Photomicrographs of a section in the skin of the control group (2A&2B) show keratinized stratified squamous epithelium of the epidermis (E), papillary (P) and reticular (R) dermis. Notice blood capillaries (thick bifid arrow), hair follicles (f) associated with sebaceous glands (s), connective tissue cells (thin bifid arrows) and fibers (arrow heads) of papillary dermis (P). (2C) shows a higher magnification for stratum basale (B) with basal oval nuclei, polyhedral cells of stratum spinosum (S) with central rounded nuclei, stratum granulosum (G) with its dark granules and stratum corneum (C) of the epidermis. Notice keratin (arrow) and keratohyalin granules (bent arrows). (H&E, 2A \times 200, 2B \times 400, 2C \times 1000)

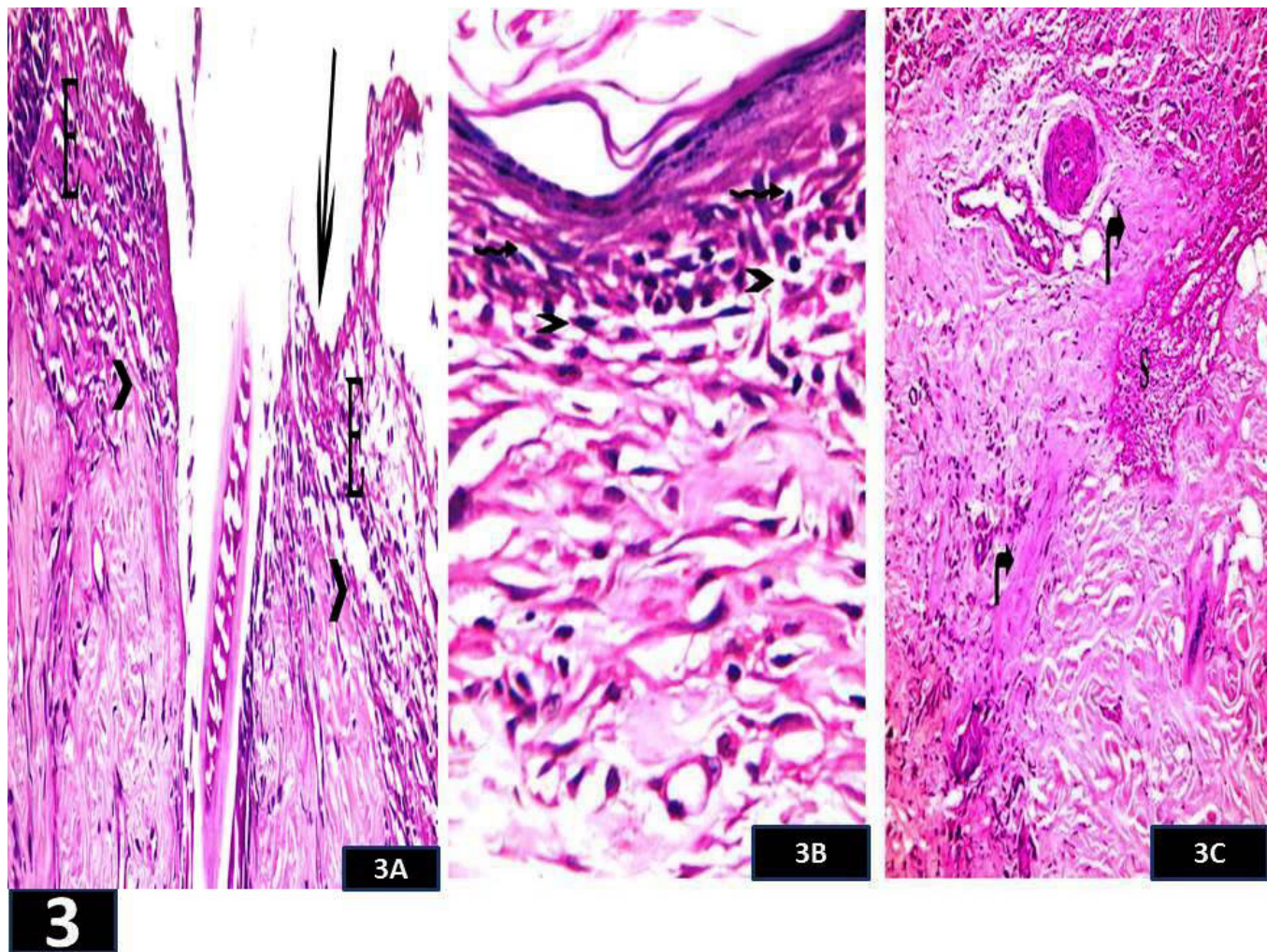


Fig. 3: Photomicrographs of a section in the skin: (3A) shows loss of definite demarcation between epidermis and dermis (>), lost epidermal strata arrangement (E), absent keratin and surface erosion (arrow). (3B) shows spaces between epidermal cells (zigzag arrows) and absent basement membrane (>). (3C) shows a homogenous acidophilic material (bent arrows) in the reticular dermis and a sebaceous gland with the proliferation of its cells (s). (Subgroup 2A, H&E, 3A $\times 400$, 3B $\times 1000$, 3C $\times 200$)

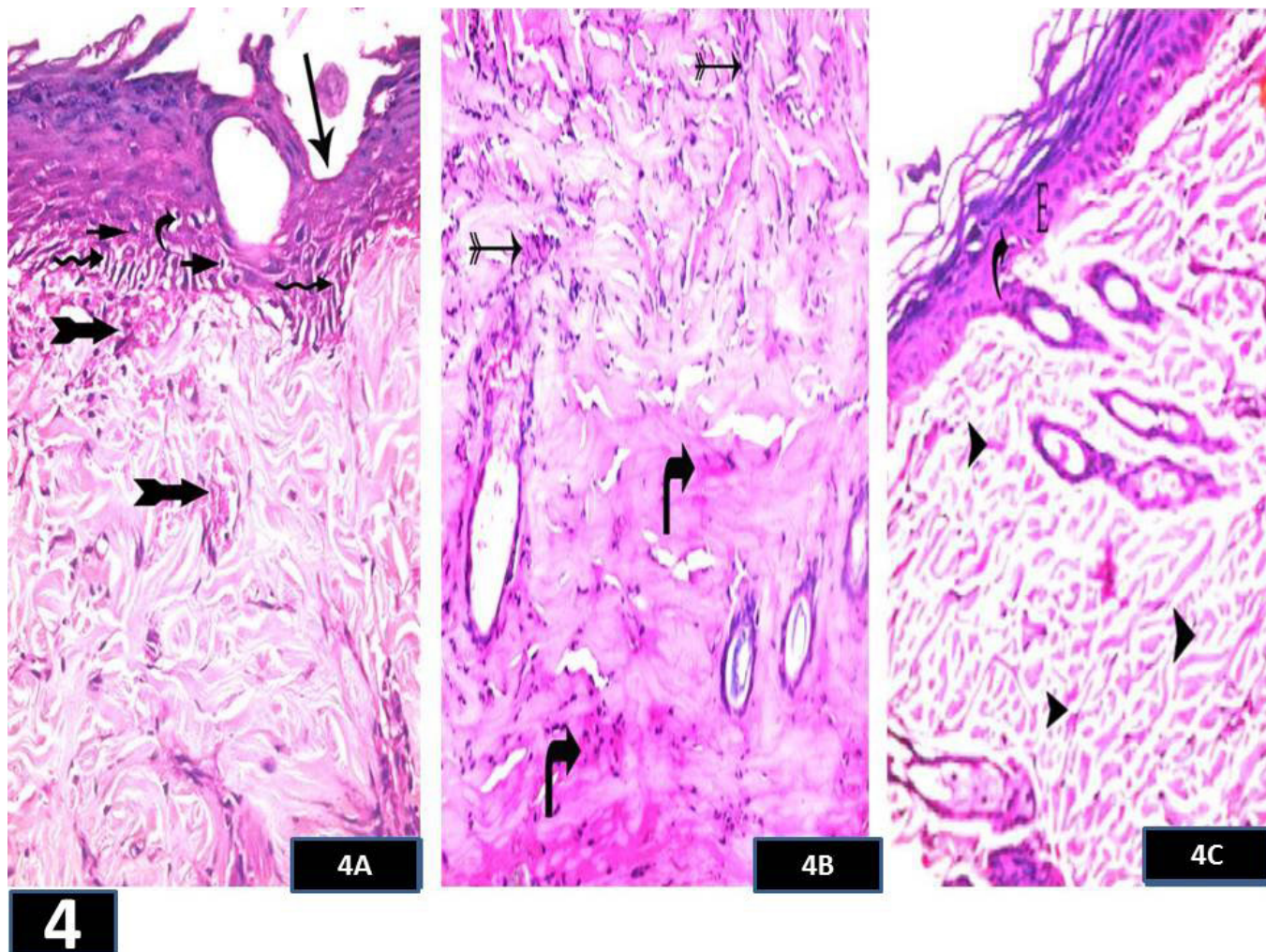


Fig. 4: Photomicrographs of a section in the skin; (4A&4B) show a skin section of subgroup 2B with marked disorganization of epidermal structures (long arrow), separation of the basal cells of epidermis (zigzag arrows), vacuolation of some epidermal cells (curved arrow) with small dark nuclei (short arrows). Notice the increased number of engorged blood vessels (thick bifid arrows), mononuclear cellular infiltration (thin bifid arrows) and homogenous acidophilic material (bent arrows) in the dermis. (4C) shows a skin section of subgroup 2C with more or less normal arrangement of four strata of the epidermis (E). A few epidermal cells show vacuolated cytoplasm and small dark nuclei (curved arrow). Notice more or less normal arrangement of fibers in the reticular dermis (arrow heads). (Subgroups 2B&2C, H&E, 4A,4B,4C $\times 400$)

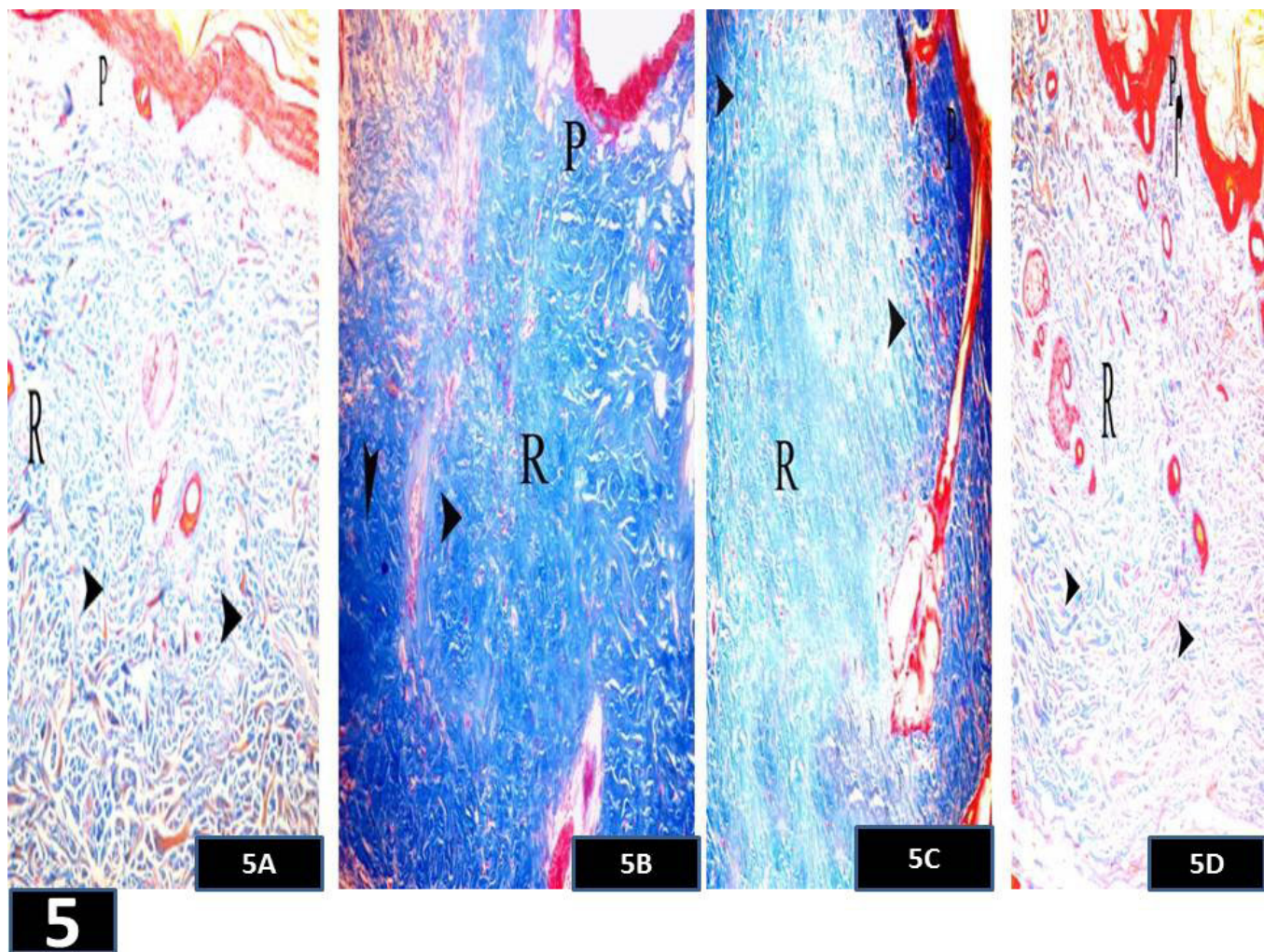


Fig. 5: Photomicrographs of sections in the skin of the control and experimental groups; (5A) shows a skin section of the control group with a fine loosely arranged network of collagen fibers in the papillary dermis (P) and thick irregular bundles (arrow heads) in the reticular layer (R). (5B) shows a skin section from subgroup 2A with an apparent increase in the thickness of collagen bundles (arrow heads) in both papillary (P) & reticular (R) dermis. (5C) shows a skin section from subgroup 2B with an apparent increase in the thickness of collagen bundles (arrow heads) in both papillary (P) & reticular (R) dermis. (5D) shows a skin section from subgroup 2C with apparent thick collagen bundles (bent arrow) in a few focal areas in the papillary dermis (P), while the reticular dermis (R) shows more or less normal arrangement of collagen bundles (arrow heads). (Mallory's trichrome stain, $\times 200$)

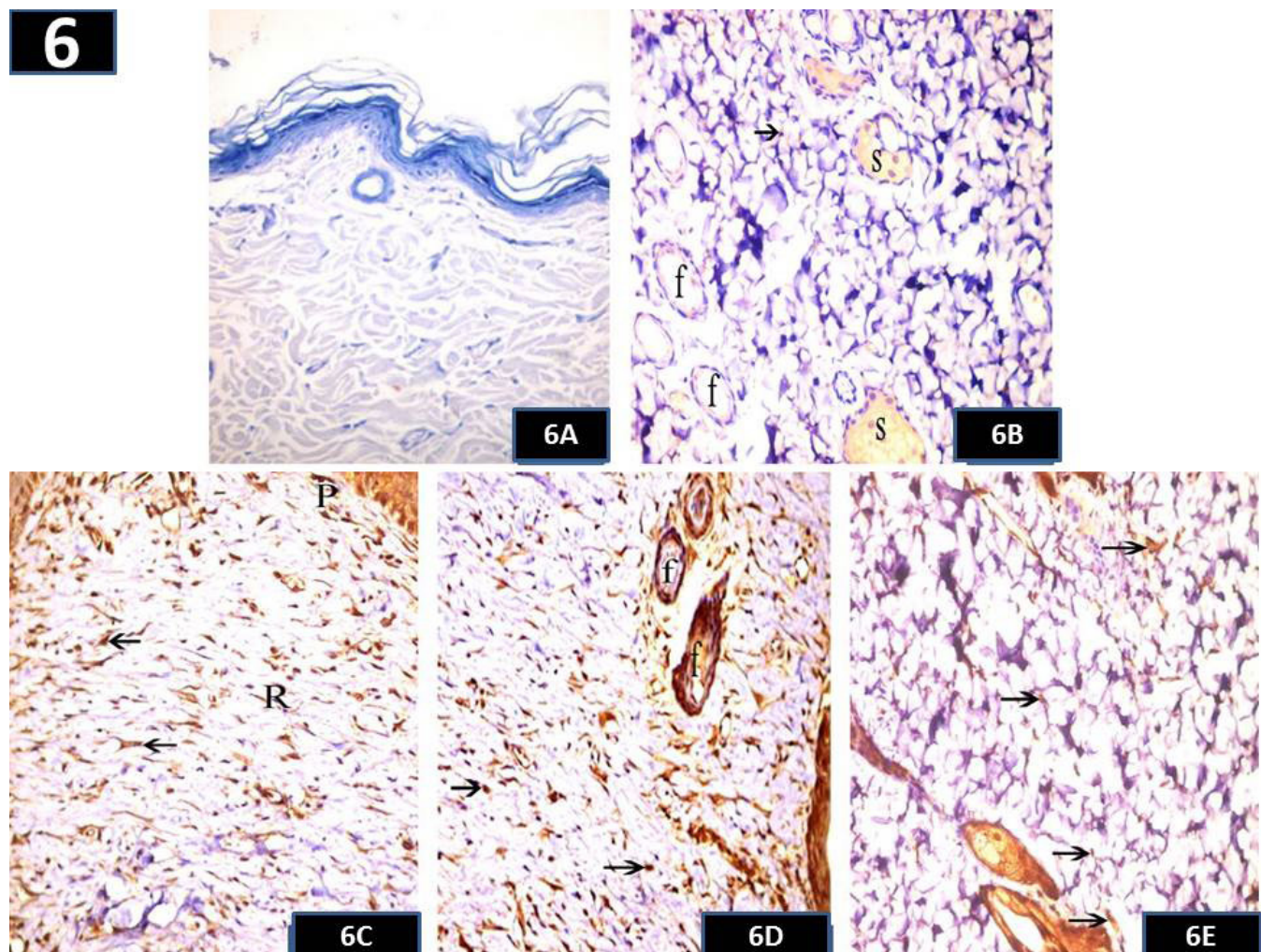


Fig. 6: Photomicrographs of sections in the skin of the control and experimental groups; (6A) shows a negative control section in the skin with negative TGF- β immunoreaction. (6B) shows a skin section from the control group with a few cells having a positive cytoplasmic immuno-reaction (arrow) in the reticular dermis. Notice a positive cytoplasmic immuno-reaction of TGF- β in the hair follicles (f) and sebaceous glands (s). (6C) shows a skin section from subgroup 2A with numerous cells (arrows) having a positive immuno-reaction (nuclear and cytoplasmic) in both papillary (P) and reticular (R) dermis. (6D) shows a skin section from subgroup 2B with numerous cells (arrows) having a positive immuno-reaction (nuclear and cytoplasmic) in the reticular dermis. Notice a positive immuno-reaction of TGF- β in the cells of hair follicles (f). (6E) shows a skin section from subgroup 2C with a few cells having a positive immuno-reaction (arrows) in the reticular dermis. (TGF- β immunostaining, $\times 400$)

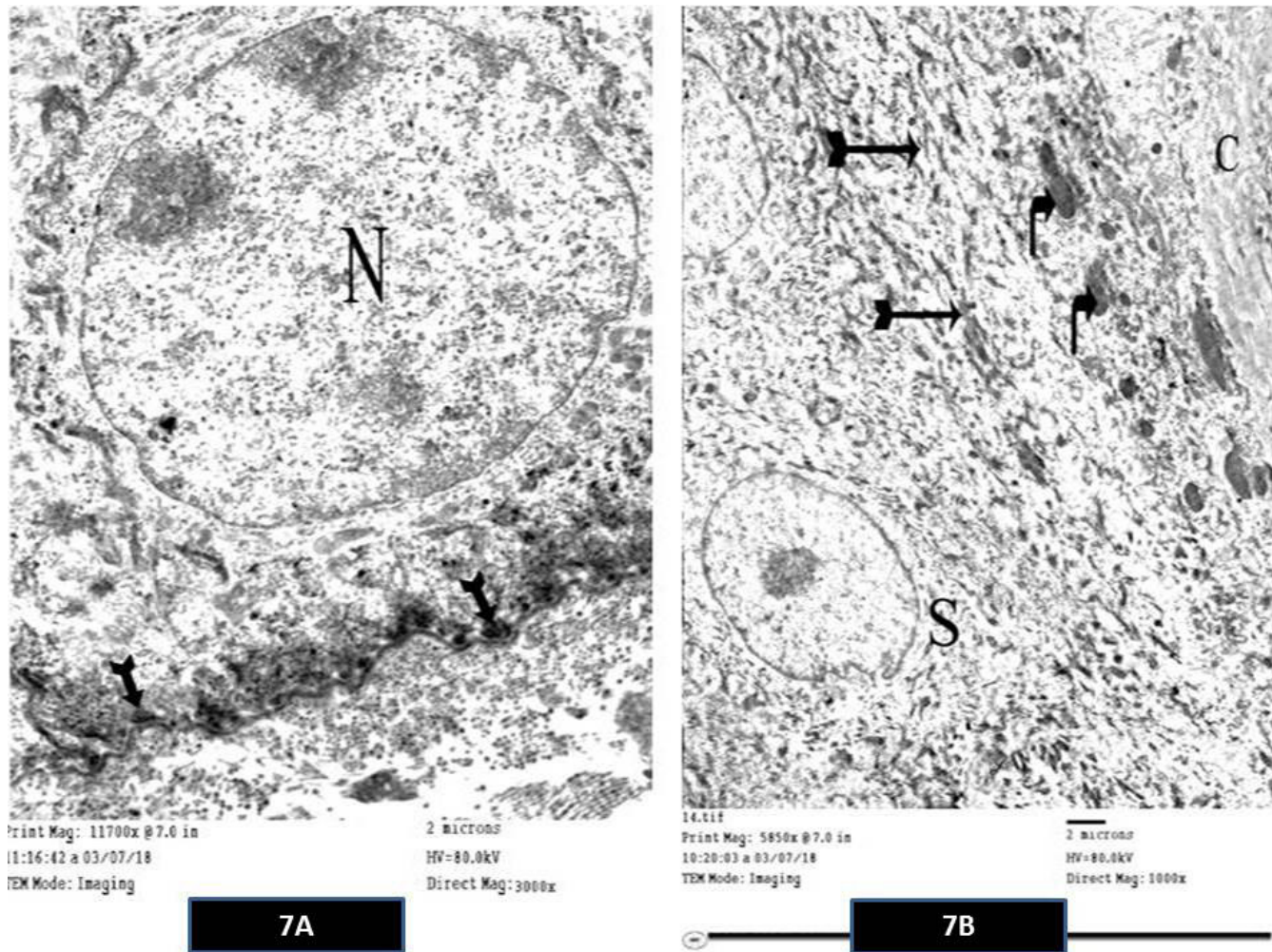


Fig. 7: Electron micrographs of the skin of the control group; (7A) shows a keratinocyte of stratum basale with an oval to rounded nucleus (N). Hemidesmosomes are noticed (bifid arrows). (7B) shows stratum spinosum (S), stratum granulosum containing keratohyalin granules (bent arrows) as well as the stratum corneum (C). Notice the tonofilaments (bifid arrows) inside the keratinocytes. (7A \times 3000, 7B \times 1000)

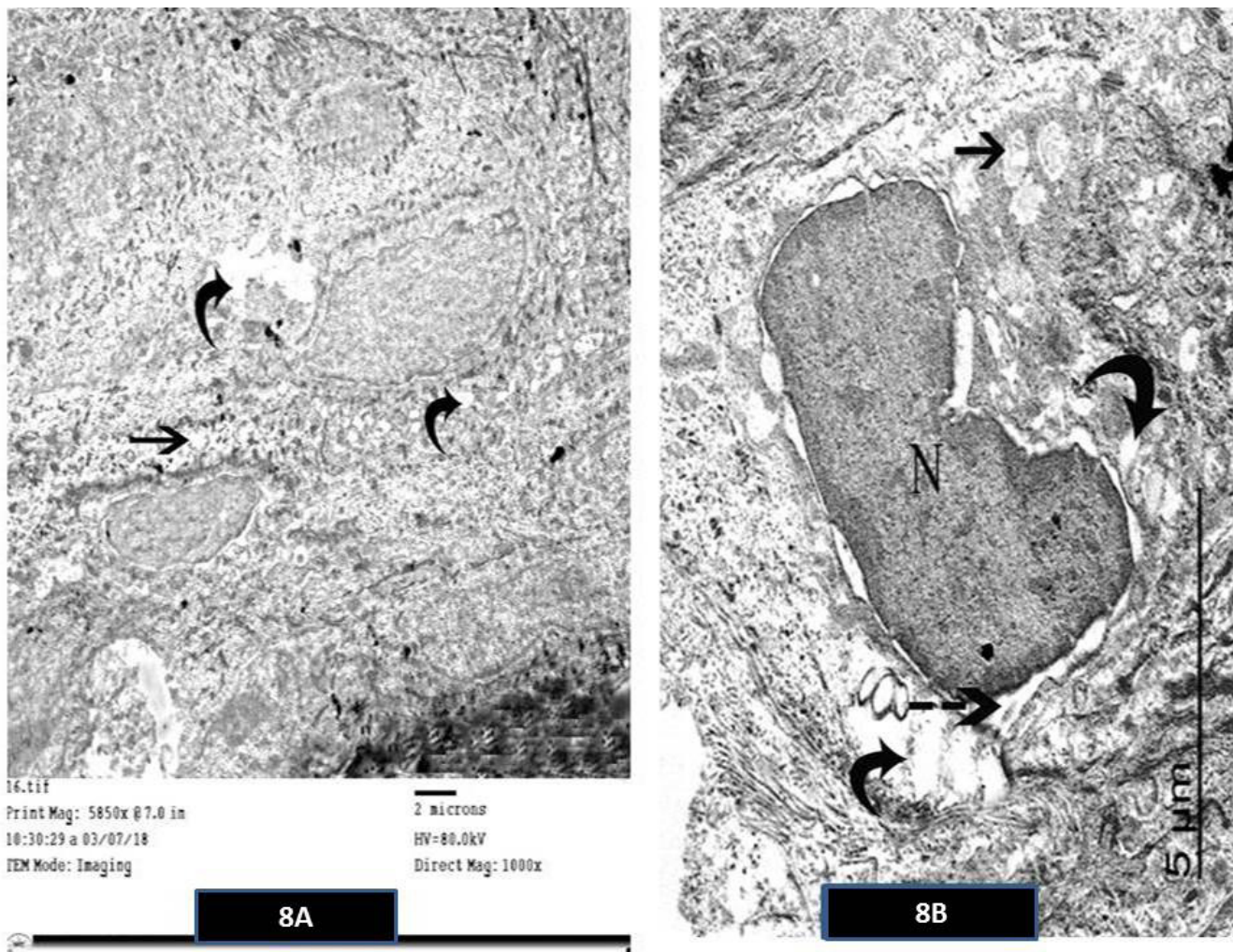


Fig. 8 (A&B): Electron micrographs of the skin of subgroup 2A show keratinocytes with vacuolated cytoplasm (curved arrows) and swollen mitochondria with disrupted cristae (arrow). Notice a keratinocyte with an irregular dark nucleus (N) and dilatation of its perinuclear space (-->). (8A \times 1000, 8B \times 1500)

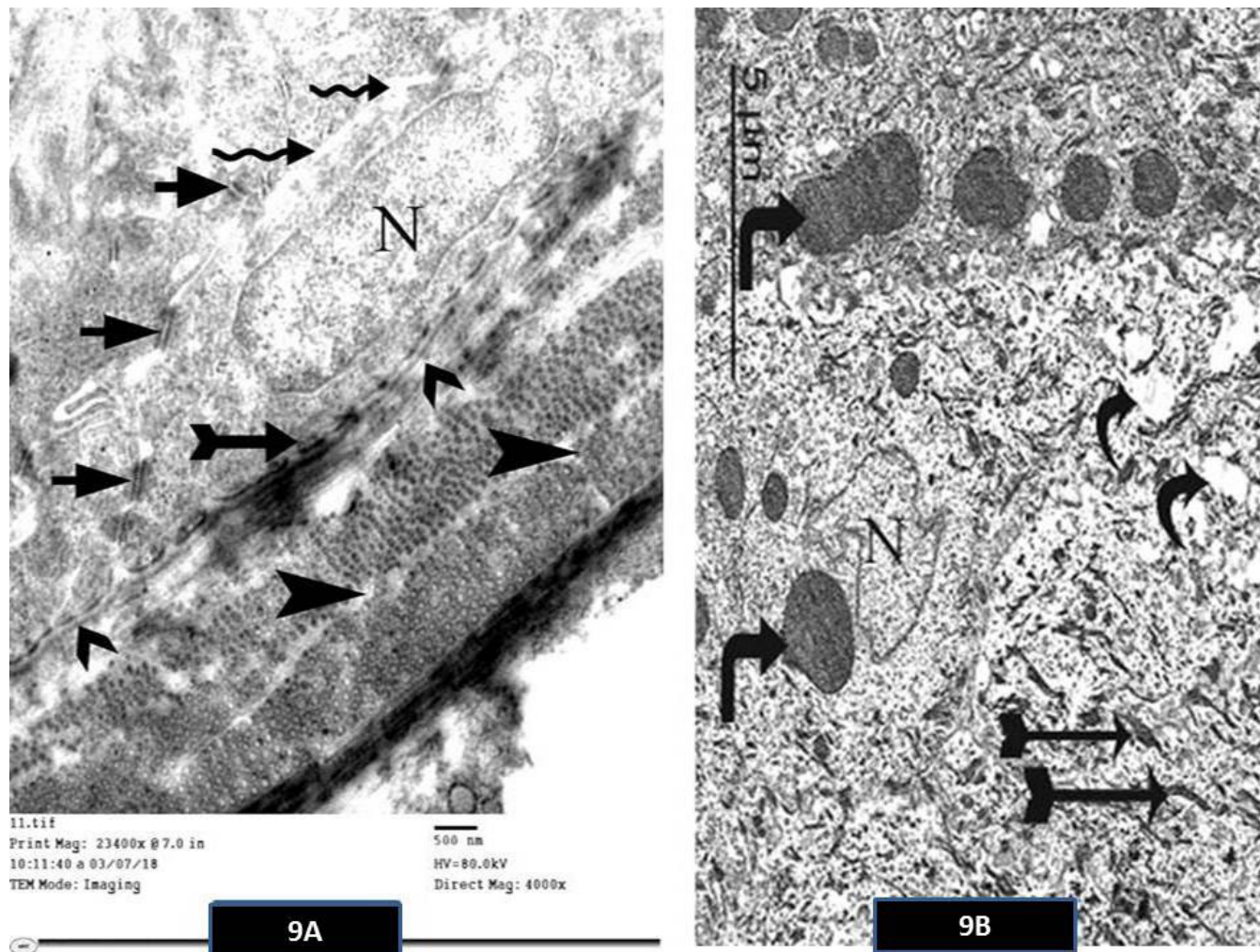


Fig. 9: Electron micrographs of the skin of subgroup 2B (9A) shows focal widening of intercellular space (zigzag arrows) with normal desmosomes (arrows) and hemidesmosomes (bifid arrow). Notice normal basement membrane (>) and abnormal arrangement of collagen fibers (arrow heads) in the papillary dermis. Abnormal transversely oriented nucleus (N) of stratum basale is noticed. (9B) shows keratinocytes of stratum granulosum with large sized keratohyalin granules (bent arrows), cytoplasmic vacuoles (curved arrows) and an irregular nucleus (N). Notice the tonofilaments (bifid arrows). (9A $\times 4000$, 9B $\times 1200$)

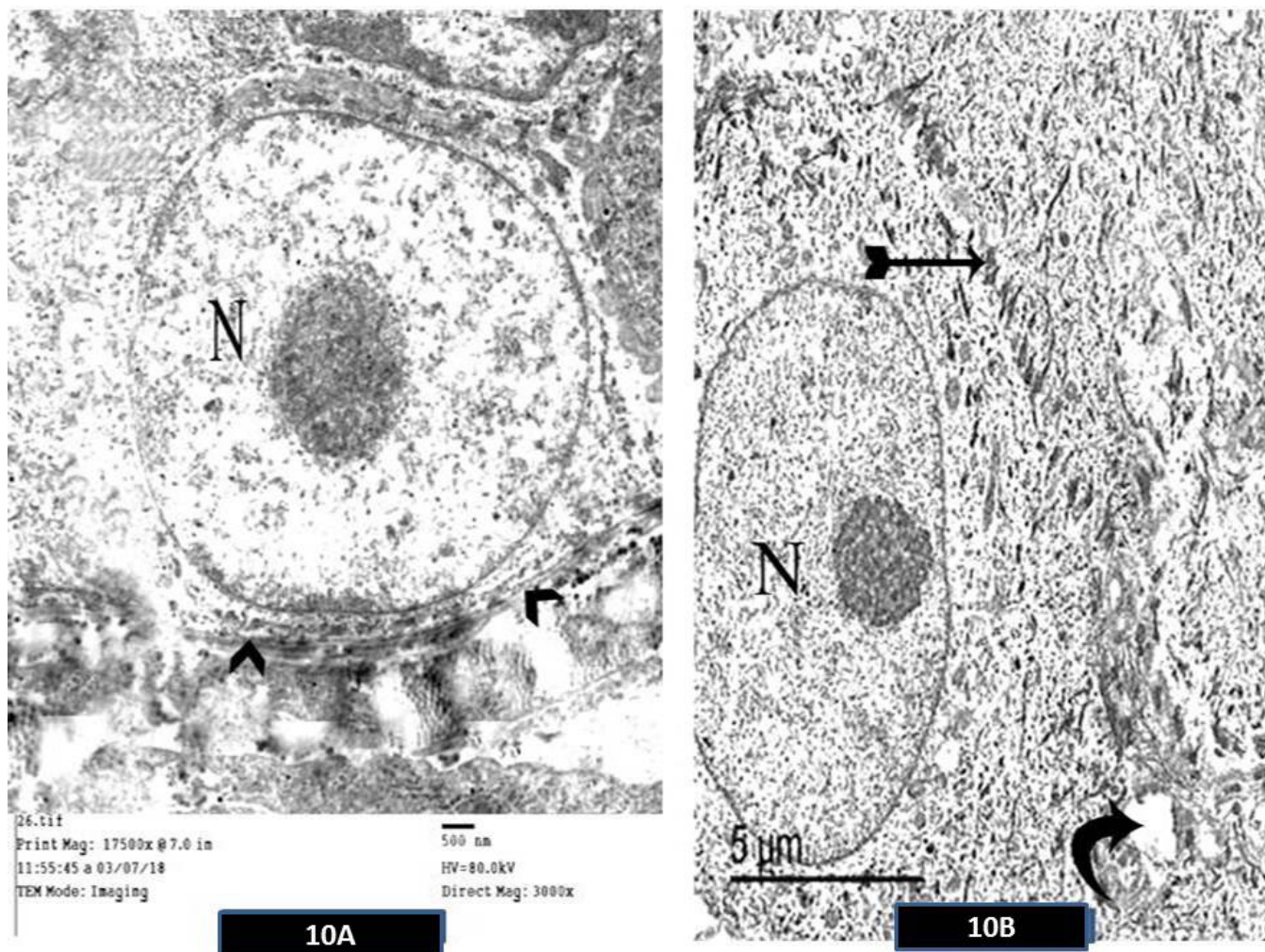
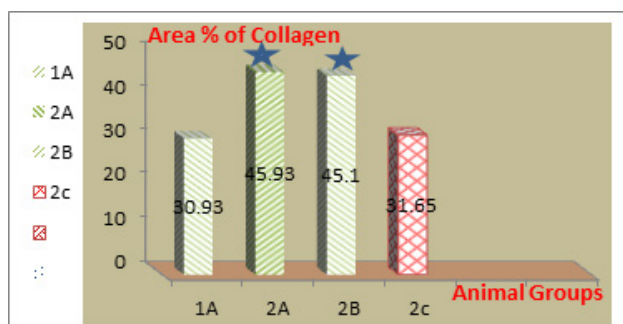
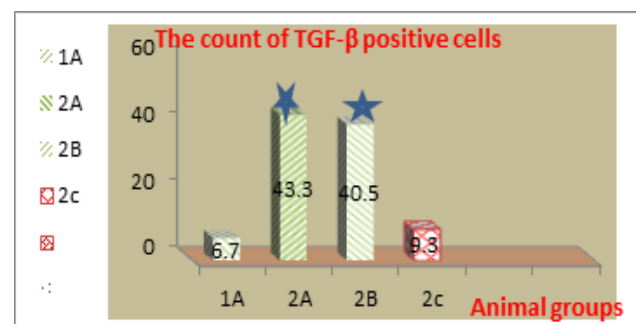


Fig. 10: Electron micrographs of the skin of subgroup 2C (10A) shows a normal nucleus of a stratum basale cell (N). Notice normal basement membrane (>), (10B) shows a keratinocyte in stratum spinosum with a few cytoplasmic vacuoles (curved arrow) and a normal nucleus (N) with a prominent nucleolus. Notice normal tonofilaments (bifid arrow). (10A × 3000, 10B × 1200)



Histogram I: Shows the surface area % of collagen



Histogram II: Shows the count of TGF-β positive cells

DISCUSSION

Bleomycin is a chemotherapeutic drug that has many side effects including skin reactions^[1,2]. So, this work was performed to study the effect of bleomycin on the structure of the skin of adult male albino rats and to evaluate the possible curative role of BM-MSCs by some histological techniques.

In this study, specimens from bleomycin-treated animals as well as bleomycin and culture media-treated groups revealed disturbance of the normal architecture of the skin. The epidermis showed lost strata arrangement and surface erosion. This was in line with other studies on bleomycin which reported that this drug induced scleroderma and caused decreased epidermal thickness in various mice strains^[23,24]. In addition, intralesional bleomycin injection is used as a line of therapy for hypertrophic scars and keloids^[25].

These epidermal structural changes may be attributed to decreased proliferation of keratinocytes. Bleomycin inhibits keratinocytes proliferation by both direct and indirect effects^[23]. The indirect effect is mediated by fibroblast-derived factors as keratinocyte growth factor or insulin-like growth factor. On the other hand, the decreased epidermal thickness may be attributed to the epidermal cell apoptosis after multiple doses of bleomycin^[24].

Specimens of animals treated with bleomycin alone as well as bleomycin and culture media-treated animals of this work showed structural changes in keratinocytes such as vacuolated cytoplasm and irregular small dark nuclei. It was suggested that the previous changes might characterize apoptotic changes^[26,27]. Bleomycin induced keratinocyte changes may be explained by the production of free radicals, reactive oxygen species (ROS) and reactive nitrogen species. Furthermore, the chelation of iron ions with oxygen leads to production of DNA-cleaving superoxide and hydroxide free radicals that lead to increased bleomycin toxicity^[28].

The present work showed focal loss of the basement membrane and loss of definite demarcation between the epidermis and dermis in bleomycin-treated animals. This was consistent with previous reports which revealed diminished basement membrane immunohistochemical reactivity to collagen monoclonal antibody and markedly decreased numbers of the anchoring fibrils^[29]. Moreover, the resulted scleroderma may cause loss of the reticular fibers (forming lamina reticularis of basement membrane) from the papillary dermis^[30]. These findings may be attributed to the destruction of reticular fibers by autoantibodies induced by bleomycin because bleomycin administration could initiate autoimmunity^[31].

Regarding the dermis, specimens of bleomycin-treated animals revealed engorged blood vessels. Anticancer drugs cause vasodilatation of dermal blood vessels and erythrocyte extravasation^[32]. In addition, cellular infiltration was noticed in the reticular dermis of bleomycin-treated

animals. This finding may be caused by an inflammatory response to bleomycin which is a prominent early finding in the fibrotic process^[33]. It was reported that bleomycin increased the numbers of neutrophils, macrophages and lymphocytes^[34]. Additionally, this may be considered as an allergic reaction induced by bleomycin which resembles atopic dermatitis^[35]. The proinflammatory cytokine S100A9 may play a role in the inflammatory process as it is a potent neutrophil chemo-attractant and can promote all types of cells to secrete inflammatory cytokines such as interleukin (IL)-6, IL-8, or tumor necrosis factor (TNF)- α ^[36].

Bleomycin-treated animals showed cellular proliferation of the sebaceous gland. This finding may be a sign of gland inflammation which occurs also in acne vulgaris^[37]. The chemotherapeutic drugs as bleomycin can induce acne form like eruption^[38].

Mallory's trichrome staining of specimens of animals treated with bleomycin alone as well as bleomycin and culture media showed an increase in the thickness of collagen bundles in both papillary and reticular dermis with subsequent decrease in the amorphous matrix in between. This was proved in our work by the morphometric and statistical study. Subcutaneous injection of bleomycin may cause increased dermal thickness as well as an increase in collagen network in a mouse model^[24,39]. This finding may be attributed to increased collagen production by fibroblasts. Increased collagen synthesis by fibroblasts is influenced by growth factors and cytokines such as transforming growth factor- β , connective tissue growth factor, endothelin-1, interleukin-4 and interleukin-6^[40]. The activation of fibroblasts may be due to reduced expression of aquaporin 3 (AQP3) compared with healthy dermal fibroblasts^[41].

Transforming growth factor- β (TGF- β) is a cytokine which is normally formed by fibroblasts of the dermis and stimulate it to synthesize collagen. It plays an important role in the formation of extracellular matrix (ECM) not only by promoting the production of collagen but also by inhibiting production of various proteases^[42]. TGF- β is inactive when it binds with decorin (a proteoglycan in the extracellular matrix) and it becomes active only when it separates from decorin^[43]. Moreover, its synthesis is increased in cases of fibrosis^[44]. By immunohistochemical technique, the control group of this study showed a few cells with a positive brown cytoplasmic immuno-reaction in the reticular dermis. On the other hand, animals treated with bleomycin alone as well as bleomycin and culture media showed numerous cells with a positive TGF- β immuno-reaction (nuclear and cytoplasmic) in the reticular dermis.

This positive TGF- β immunoreaction represents fibroblasts and myofibroblasts^[45]. The increased number of positive fibroblasts and myofibroblasts may be attributed to increased synthesis of TGF- β by them^[46]. TGF- β is responsible for increases the synthesis of collagen by fibroblasts^[47]. Furthermore, TGF- β is capable of stimulating

its own synthesis by fibroblasts through autoinduction^[48]. Moreover, myofibroblasts are also activated during fibrosis by connective tissue growth factor (CTGF), autocrine factors and paracrine signals derived from lymphocytes and macrophages^[49].

It was noticed that TGF- β immuno-reaction in the control group of this research appeared in the cytoplasm of a few positive cells in the dermis, while it appeared both cytoplasmic and nuclear in animals treated with bleomycin alone as well as in bleomycin and culture media. Regarding the fibroblasts, TGF- β binds to type II serine/threonine kinase receptor (in the cell membrane)^[50]. Type II kinase receptor phosphorylates and activates type I kinase receptor that activates a signaling cascade which is able to carry TGF- β and translocate it into the nucleus^[51]. So, the reaction appears nuclear with increased production of TGF- β .

Ultrastructurally, swollen mitochondria with disrupted cristae, irregular nuclei and dilated perinuclear spaces were observed in keratinocytes of animals treated with bleomycin alone as well as bleomycin and culture media. These changes may be attributed to ROS and oxidative stress that may lead to apoptosis^[52]. The mitochondria contain several proteins, including cytochrome C. These proteins are capable of activating apoptotic pathways. ROS lead to the formation of a channel called the mitochondrial permeability transition pore. The opening of this channel results in swelling of mitochondria and failure of oxidative phosphorylation leading to progressive adenosine triphosphate (ATP) depletion. The increased permeability of mitochondrial membrane as a result of its damage may result in leakage of these proteins into the cytosol and the death of the cell^[53].

Our study also showed large sized keratohyalin granules in cells of the stratum granulosum of the bleomycin-treated animals. This finding could be explained by stimulation of the keratinocytes to protect themselves against the harmful effect of bleomycin. Keratinocytes can be directly activated by a large number of exogenous stimuli as UV rays, infectious agents or exogenous chemicals^[54]. Moreover, keratohyalin granules help in the protection of the cells beneath them from radiation. In addition, this change may be attributed to oxidative stress and the production of free radicals such as reactive oxygen species superoxides, hydrogen peroxides, and hydroxyl radicals which cause keratinocytes damage^[55,56].

Focal widening of the intercellular spaces was observed ultrastructurally in bleomycin and culture media-treated animals of this study. This could be explained by splitting of desmosomes and loss of cell to cell contact^[57].

Our study also revealed that BM-MSCs partially improved the structural changes induced by bleomycin in the epidermis of the skin. The epidermis showed the normal arrangement of its four strata with nearly normal cellular architecture. It was reported that MSCs could induce epidermal regeneration in cutaneous injury^[58,59].

This may be attributed to the role of MSCs in promoting keratinocytes proliferation and inhibition of their apoptosis by decreased expression of the oxidant-associated marker as malondialdehyde (MDA) and increased the antioxidant enzymes as superoxide dismutase (SOD) and glutathione peroxidase (GSH-Px)^[60]. Moreover, MSCs can be differentiated into keratinocytes during wound healing^[61].

The dermis also showed improvement of the structural changes induced by bleomycin due to BM-MSCs. Collagen fibers appeared more or less with normal arrangement by Mallory's trichrome stain. This improvement of fibrosis was attributed to the antifibrotic paracrine effects of MSCs modulating fibroblasts proliferation and prevention of collagen accumulation by mediating TGF- β -dependent activation^[62]. The improvement of dermal fibrosis may be due to the immunomodulatory effects of MSCs^[63]. BM-MSCs can significantly reduce fibrotic skin contracture and collagen accumulation in a murine model^[64]. It was reported that MSCs can improve fibrosis of many body organs as heart, pancreas, colon, rectum, peritoneum, kidneys, liver and lung as well as radiation-induced scleroderma^[65-68].

Absence of the inflammatory cells was observed in sections of bleomycin and MSCs-treated animals. This may be attributed to the ability of MSCs to inhibit the inflammatory process which precedes fibrosis^[69].

The protective effect of MSCs on bleomycin-induced scleroderma was recorded in mice, and it was found that MSCs may facilitate the degradation and remodeling of ECM through the production of higher levels of metalloproteinases (MMPs)-2, -9 and -13^[70]. In addition, MSCs can restore the levels of matrix proteins as decorin which is involved in wound healing. Decorin is the most abundant proteoglycan in normal dermis which promotes the lateral association of collagen fibrils to form fibers and fiber-bundles. Decorin insufficiency leads to a delay in cutaneous wound healing^[71].

Immunohistochemically, bleomycin and MSCs-treated animals showed a few cells with positive TGF- β immunoreaction in the reticular dermis. This finding was enforced by the morphometric and statistical study. It may be attributed to decreased production of TGF- β by fibroblasts and myofibroblasts^[72]. MSCs can restore decorin which binds to TGF- β inactivating it^[43,71].

CONCLUSION AND RECOMMENDATIONS

Bleomycin has harmful effects on the skin of adult male albino rats. It altered the histological structure of the epidermis and induced dermal fibrosis through increasing the expression of TGF- β . BM-MSCs improved these epidermal structural changes and ameliorated dermal fibrosis by decreasing the expression of TGF- β . This is indicative of the curative role of BM-MSCs against bleomycin-induced skin damage in rats. So, BM-MSCs may be used to minimize skin complications in clinical cases of bleomycin therapy. Further animal studies were recommended to evaluate the effect of bleomycin and BM-MSCs on the proliferative capacity of the epidermis.

CONFLICT OF INTERESTS

There are no conflicts of interest.

REFERENCES

- Reinert T, Serodio C, Baldotto D, Nunes F, Scheliga A (2013): Bleomycin-Induced Lung Injury. *Journal of Cancer Research* 10: 1155-1164.
- Bhushan P, Manjul P, Baliyan V (2014): Flagellate dermatosis. *Indian J Dermatol Venereol Leprol.* 80:149-152.
- Avouac J (2014): Mouse model of experimental dermal fibrosis: the bleomycin induced dermal fibrosis. *Methods Mol Biol.* 1142: 91-98.
- Resende C, Araujo C, Gomes J, Brito C (2013): Bleomycin-induced flagellate hyperpigmentation. *BMJ Case Reports* 10: 31-36.
- Orciani M, Campanati A, Salvolini E, Lucarini G, Di Benedetto G, Offidani A, Di Primo R (2011): The mesenchymal stem cell profile in psoriasis. *Br J Dermatol.* 165: 585-592.
- Wu Y, Huang S, Enhe J, Ma K, Yang S, Sun T, Fu X, (2013): Bone marrow-derived mesenchymal stem cell attenuates skin fibrosis development in mice. *Int Wound J.* 11: 701-710.
- Li Y, Yan B, Wang H, Li H, Li Q, Zhao D, Chen Y, Zhang Y, Li W, Zhange J, Wang S, Shen J, Li Y, Guindi E, Zhao Y (2015): Hair regrowth in alopecia areata patients following Stem Cell Educator therapy. *BMC medicine* 13: 1015-1033.
- Al-Dhamin Z, Liu LD, Li DD, Zhang SY, Dong SM, Nan YM (2020): Therapeutic efficiency of bone marrow-derived mesenchymal stem cells for liver fibrosis: A systematic review of *in vivo* studies. *World J Gastroenterol.* 26(47): 7444-7469.
- Juniantito V, Izawa T, Yuasa T, Ichikawa C, Yano R, Kuwamura M, Yamate J (2013): Immunophenotypical characterization of macrophages in rat bleomycin-induced scleroderma. *Vet pathol.* 50: 76-85.
- Maria A, Toupet K, Bony C, Pirot N, Vozenin M, Petit B, Roger P, Batteux F, Quellec A, Jorgensen C, Noel D, Guilpain P (2016): Antifibrotic, Antioxidant, and Immunomodulatory Effects of Mesenchymal Stem Cells in HOCl-Induced Systemic Sclerosis. *Arthritis Rheumatol.* 68(4): 1013-1025.
- Gaertner DJ, Hallman TM, Hankenson FC, Batcherder MA (2008): Anesthesia and Analgesia in Rodents. *Anesthesia and analgesia in laboratory animals.* 2nd edition. Academic Press, San Diego, CA. Boston. P: 239-240.
- Huang S, Xu L, Sun Y, Wu T, Wang K, Li G (2015): An improved protocol for isolation and culture of mesenchymal stem cells from mouse bone marrow. *Journal of Orthopaedic Translation* 3: 26-33.
- McFarlin K, Gao X, Liu Y, Dulchavsky D, Kwon D, Arbab A, Bansal M, Chopp M, Dulchavsky SA, Gautam S (2006): Bone marrow-derived mesenchymal stromal cells accelerate wound healing in the rat. *Wound Repair Regen.* 14: 471-478.
- Yang E, Liu N, Tang Y, Hu Y, Zhang P, Pan C, Dong S, Zhang Y, Tang Z (2015): Generation of Neurospheres from Human Adipose-Derived Stem Cells. *Biomed Res Int.*; 2015: 714-737.
- Piccinini F, Tesei A, Arienti C, Bevilacqua A (2017): Cell Counting and Viability Assessment of 2D and 3D Cell Cultures: Expected Reliability of the Trypan Blue Assay; *Biological Procedures Online* 19: 1186-1194.
- Patel H, Chudasma A, Patel N (2014): *In-Vitro* Cytotoxicity Studies for Calcium Coated Liposome. *IJPRBS*; 3: 581-590.
- Bancroft J, Christophe L, kim S (2013): *Bancroft's theory and practice of histological techniques.* 7th edition, Churchill Livingstone. P:179-202.
- Bozzola JJ and Russell LD (1999). *Electron microscopy: principles and techniques for biologists,* 2nd edition, Jones and Bartlett Publishers. P: 100-124.
- Kumar Gand Rudbeck L (2009): *Immunohistochemical (IHC) Staining Methods.* 5th edition. Lippincott Williams & Wilkins. California. P. 57-61.
- Jurukovski V, Dabovic B, Todorovic V, Chen Y (2015): Methods for Measuring TGF- β Using Antibodies, Cells, and Mice. *Methods in molecular medicine*; 117:161-175.
- Elgendy MS, Elsayed AM, Eldosokey DE, Abd Elmaqsoud AK (2021): Histological and Immunohistochemical Study to Evaluate the Effects of Metformin versus Green Tea Extracts on Bleomycin Induced Lung Injury In Adult Male Albino Rats. *EJH.* 44(1): 31-47.
- Fedchenko N and Reifenrath J (2014): Different approaches for interpretation and reporting of immunohistochemistry analysis results in the bone tissue – a review. *Diagn Pathol.* 9: 221.
- Yamamoto T, Kuroda M, Nishioka K (2000): Animal model of sclerotic skin. III: Histopathological comparison of bleomycin-induced scleroderma in various mice strains. *Dermatol Res.* 292: 535-541.
- Ould-Ali D, Hautier A, Andrac-Meyer L, Bardin N, Magalon G, Granel B (2012): Bleomycin-induced Scleroderma in Nude Mice can be Reversed by Injection of Adipose Tissue: Evidence for a Novel Therapeutic Intervention in Systemic Sclerosis. *J Clin Exp Dermatol Res.* 3:164- 174.
- Payapvipapong K, Niumpradit N, Piriyanand C, Buranaphalin S, Nakakes A (2015): The Treatment of keloids and hypertrophic scars with intralesional bleomycin in skin of color. *J Cosmet Dermatol.* 14:83-90.

26. Bottone M, Santin G, Aredia F, Bernocchi G, Pellicciari C, Scovassi A (2013): Morphological Features of Organelles during Apoptosis: An Overview. *Cells* 2: 294-305.
27. Zhang Y, Chen X, Gueydan C, Han J (2018): Plasma membrane changes during programmed cell deaths. *Cell Research*; 28: 9-21.
28. Mousa AM (2016): Effect of Pirfenidone on Bleomycin Induced Pulmonary Alveolar Fibrosis in Adult Male Rats (Histological, Immunohistochemical, Morphometrical and Biochemical Study). *International Journal of Clinical and Developmental Anatomy*; 2: 17-23.
29. Ishikawa O, Warita S, Ohnishi K, Miyachi Y (1993): A scleroderma-like variant of recessive dystrophic epidermolysis bullosa. *Br J Dermatol.* 129: 602-605.
30. Gabriela E, Raica M, Anca M, Viorica B (2007): Morphologic and histochemical changes in the skin of patients with scleroderma. *Romanian Journal of Morphology and Embryology*; 28: 361-367.
31. Ishikawa H, Takeda K, Okamoto A, Matsuo S (2009): Induction of Autoimmunity in a Bleomycin-Induced Murine Model of Experimental Systemic Sclerosis: An Important Role for CD4+ T Cells. *J Invest Dermatol.* 129: 1688-1695.
32. Selleri S, Seltmann H, Gariboldi S, Shirai Y, Balsari A, Christos C, Rumio C (2006): Doxorubicin-Induced Alopecia Is Associated with Sebaceous Gland Degeneration. *J Invest Dermatol.* 126: 711-720.
33. Wu M, Denisa S, Chang E, Warner-Blankenship M, Ghosh A, Varga J (2009): Rosiglitazone abrogates bleomycin-induced scleroderma and blocks profibrotic responses through peroxisome proliferator-activated receptor. *Am J Pathol.* 174: 519-533.
34. Gao L, Tang H, He H, Liu J, Mao J, Ji H, Lin H, Wu T, (2015): Glycyrrhizic acid alleviates bleomycin-induced pulmonary fibrosis in rats. *Front Pharmacol.* 6: 215-222.
35. Sung Y, Kim S, Yang W, Park Y, Kim H (2018): Bleomycin Aggravates Atopic Dermatitis via Lung Inflammation in 2,4-Dinitrochlorobenzene-Induced NC/Nga Mice. *Front Pharmacol.* 2018: 578-587.
36. Xu X, Chen Z, Zhu X, Wang D, Liang J, Zhao C, Feng X, Wang J, Zou H, Sun L (2018): S100A9 aggravates bleomycin-induced dermal fibrosis in mice via activation of ERK1/2 MAPK and NF- κ B pathways. *Iran J Basic Med Sci.* 21: 194-201.
37. Makrantonaki E, Ganceviciene R, Zouboulis C (2011): An update on the role of the sebaceous gland in the pathogenesis of acne. *Dermatoendocrinol.* 3: 41-49.
38. Priyadarshini C, Mohapatra J, Sahoo T, Pattnaik S (2016): Chemotherapy Induced Skin Toxicities and Review of Literature. *Journal of Cancer and Tumor International*; 3: 1-16.
39. Tanaka C, Fujimoto M, Hamaguchi Y, Sato S, Takehara K, Hasegawa M, (2010): Inducible Costimulator Ligand Regulates Bleomycin-Induced Lung and Skin Fibrosis in a Mouse Model Independently of the Inducible Costimulator/Inducible Costimulator Ligand Pathway. *Arthritis Rheum.* 62: 1723-1732.
40. Walters R, Pulitzer M, Kamino H (2009): Elastic fiber pattern in scleroderma/Morphea. *J Cutan Pathol.* 22: 617-620.
41. Yousefi B, Mahmoudi M, Sarafnejad A, Karimizadeh E, Farhadi E, Jamshidi A, Kavosi H, Aslani S, Gharibdoost F (2017): Downregulation of Aquaporin3 in Systemic Sclerosis Dermal Fibroblasts. *Iran J Allergy Asthma Immunol.* 16: 228-234.
42. Liarte S, Bernabe-Garcia A, Nicolas FJ (2020): Role of TGF- β in Skin Chronic Wounds: A Keratinocyte Perspective. *Cells* 9(2):306.
43. Hirose T, Ogura T, Tanaka K, Takehana K (2015): Comparative study of dermal components and plasma TGF- β 1 levels in Slc39a13/Zip13 -KO mice. *Journal of Veterinary Medical Science*; 77: 92-113.
44. Tracy L, Minasian R, Caterson E (2016): Extracellular Matrix and Dermal Fibroblast Function in the Healing Wound. *Adv Wound Care* 5: 119-136.
45. Takagawa S, Lakos G, Mori Y, Varga J, Yamamoto T, Nishioka K (2003): Sustained Activation of Fibroblast Transforming Growth Factor- β /Smad Signaling in a Murine Model of Scleroderma. *J Invest Dermatol.* 121: 41-50.
46. Frangogiannis NG (2020): Transforming growth factor- β in tissue fibrosis. *J Exp Med.* 217(3): e20190103: 1-16.
47. Shibusawa Y, Negishi I, Tabata Y, Ishikawa O (2008): Mouse model of dermal fibrosis induced by one-time injection of bleomycin-poly (L-lactic acid) microspheres. *Rheumatology*; 47: 454-457.
48. Jelaska A and Korn J (2000): Role of apoptosis and transforming growth factor beta1 in fibroblast selection and activation in systemic sclerosis. *Arthritis Rheum.* 43: 2230-2239.
49. Varkey M, Ding J, Tredget E (2015): Advances in Skin Substitutes—Potential of Tissue Engineered Skin for Facilitating Anti-Fibrotic Healing. *J Funct Biomater.* 6: 547-563.
50. Mori S, Chen S, Varga J (2003): Expression and Regulation of Intracellular SMAD Signaling in Scleroderma Skin Fibroblasts. *Arthritis Rheum.* 48: 1964-1978.
51. Heldin C and Moustakas A (2016): Signaling receptors for TGF- β family members. *Cold Spring Harb Perspect Biol.* 8(8), a 022053:1-33.

52. Stevens A and Lowe J (2000): Pathology. 2nd edition. Mosby, London. P. 26.
53. Kumar V, Abbas A, Fausto N, Mitchell R (2007): Robbins Basic Pathology. 9th edition. Saunders Elsevier. Philadelphia. P. 15.
54. Yel M, Güven T, Türker H (2014): Effects of ultraviolet radiation on the stratum corneum of skin in mole rats. Journal of radiation research and applied science 7: 506-511.
55. Arron S (2016): Anatomy of the Skin and Pathophysiology of Radiation Dermatitis. Skin Care in Radiation Oncology; 1007: 9-14.
56. Sarzi-Puttini P, Doria A, Girolomoni G, Kuhn A (2006): Handbook of systemic autoimmune diseases. 1st edition. Elsevier. Amsterdam. P: 5.
57. Brooke M, Nitoiu D, Kelsel D (2012): Cell-cell connectivity: desmosomes and disease. J Pathol. 226: 158-171.
58. Wu Y, Zhao R, Tredget E (2010): Concise review: bone marrow-derived stem/progenitor cells in cutaneous repair and regeneration. Stem Cells; 28: 905-915.
59. Aoki S, Toda S, Ando T, Sugihara H (2004): Bone Marrow Stromal Cells, Preadipocytes, and Dermal Fibroblasts Promote Epidermal Regeneration in Their Distinctive Fashions. Mol Biol Cell. 15: 4647-4657.
60. Liu Z, Hu G, Luo X, Yin B, Shu B, Guan J, Jia C (2017): Potential of bone marrow mesenchymal stem cells in rejuvenation of the aged skin of rats. Biomed Rep. 6: 279-284.
61. Isakson M, Blacam C, Whelan D, McArdle A, Clover A (2015): Mesenchymal Stem Cells and Cutaneous Wound Healing: Current Evidence and Future Potential. Stem Cells Int. 2015: 1155-1165.
62. Wu Y, Peng Y, Gao D, Feng C, Yuan X, Li H, Wang Y, Yang L, Huang S, Fu X (2015): Mesenchymal stem cells suppress fibroblast proliferation and reduce skin fibrosis through a TGF- β 3-dependent activation. Int J Low Extrem Wounds 14: 50-62.
63. Zhao Q, Hongying H, Han Z (2016): Mesenchymal stem cells: Immunomodulatory capability and clinical potential in immune diseases. Journal of Cellular Immunotherapy 2 (1): 3-20.
64. Horton J, Hudak K, Chung E, White A, Scroggins B (2013): Mesenchymal Stem Cells Inhibit Cutaneous Radiation-Induced Fibrosis by Suppressing Chronic Inflammation. Stem Cells 31: 2231-2241.
65. Zhuang Q, Ma R, Yin Y, Lan T, Yu M, Ming Y (2019): Mesenchymal Stem Cells in Renal Fibrosis: The Flame of Cytotherapy. Stem Cells Int. Volume 2019, Article ID; 8387350:1-18.
66. Usunier B, Benderitter M, Tamarat R, Chapel A (2014): Management of Fibrosis: The Mesenchymal Stromal Cells Breakthrough. Stem Cells Int. 2014: 1155-1165.
67. Li X, Yue S, Luo Z (2017): Mesenchymal stem cells in idiopathic pulmonary fibrosis. Oncotarget 8: 600-616.
68. Milosavljevic N, Gazdic M, Markovic B, Arsenijevic A, Nurkovic J, Dolicanin Z, Jovicic N, Jeftic I, Djonov V, Arsenijevic N, Lukic M, Volarevic V (2018): Mesenchymal stem cells attenuate liver fibrosis by suppressing Th17 cells - an experimental study. Transpl Int. 31: 102-115.
69. Haddad R and Araujo F (2014): Mechanisms of T-Cell Immunosuppression by Mesenchymal Stromal Cells: What Do We Know So Far? Biomed Res Int. 2014: 1-14.
70. Wu Y, Huang S, Enhe J, Ma K, Yang S, Sun T, Fu X (2014): Bone marrow-derived mesenchymal stem cell attenuates skin fibrosis development in mice. Int Wound J. 11: 701-710.
71. Linard C, Brachet M, Strup-Perrot C, L'homme B, Busson E, Squiban C, Holler V, Bonneau M, Lataillade J, Bey E, Benderitter M (2018): Autologous Bone Marrow Mesenchymal Stem Cells Improve the Quality and Stability of Vascularized Flap Surgery of Irradiated Skin in Pigs. Stem Cells Transl Med. 7: 569-582.
72. El Agha E, Kramann R, Schneider R, Li X, Seeger W, Humphreys B, Bellusci S (2017): Mesenchymal Stem Cells in Fibrotic Disease. Cell Stem Cell; 21: 166-177.

المخلص العربي

الدور العلاجي المحتمل للخلايا الجذعية الميزنشيمية المشتقة من نخاع العظم في التغيرات الجلدية التي يسببها البليوميسين في ذكور الجرذان البيضاء البالغة

أمل على عبد الحافظ، مرام محمد الكيلاني، أماني محمد ابراهيم موسى، ثريا عبد العزيز الديب،
أميرة عدلى كساب

قسم الهستولوجيا، كلية الطب، جامعة طنطا، مصر

المقدمة: البليوميسين هو علاجي كيميائي تم استخدامه في علاج العديد من الأورام. يؤدي تطبيقه إلى آثار جانبية جلدية مختلفة. تم إثبات دور الخلايا الجذعية الميزنشيمية المشتقة من نخاع العظم في تجديد الأنسجة.

الهدف من الدراسة: دراسة تأثير البليوميسين على التركيب النسيجي لجلد ذكور الجرذان البيضاء البالغة وتقييم الدور العلاجي المحتمل للخلايا الجذعية الميزنشيمية المشتقة من نخاع العظم.

مواد وطرق البحث: تم تقسيم خمسة وأربعين من ذكور الجرذان البيضاء البالغة إلى مجموعتين. ضمت المجموعة الضابطة ١٥ جرذاً. ضمت المجموعة التجريبية ٣٠ جرذاً وتم تقسيمها إلى ثلاث مجموعات فرعية متساوية: ٢A ، ٢B ، ٢C. تم حقن جرذان المجموعة التجريبية بالبليوميسين تحت الجلد لمدة أربعة أسابيع. تلقى كل جرذاً من المجموعة الفرعية ٢A [٠,١] مجم [من بليوميسين. تلقى كل جرذاً من المجموعة الفرعية ٢B [١] مل [من وسائط زراعة خلايا نخاع العظم بعد يوم واحد من آخر جرعة بليوميسين. تلقى كل جرذاً من المجموعة الفرعية ٢C (٢,٥ × ١٠٦) الخلايا الجذعية الميزنشيمية المشتقة من نخاع العظم بعد يوم واحد من آخر جرعة بليوميسين. تم فحص عينات الجلد بالمجهر الضوئي والإلكتروني. تم إجراء دراسة هستوكيميائية مناعية باستخدام الأجسام المضادة لتحويل عامل النمو بيتا (TGF-β). تم إجراء تقييم لنسبة مساحة سطح الكولاجين وعدد الخلايا الموجبة لـ TGF-β.

النتائج: أظهرت المجموعتان الفرعيتان التجريبيتان ٢A و ٢B اضطراباً في التركيب الطبيعي للجلد. كانت هناك زيادة كبيرة في نسبة مساحة سطح الكولاجين وعدد الخلايا الموجبة لـ TGF-β. وعلى مستوى البنية التحتية ، أظهرت بعض الخلايا الكيراتينية تجاوزاً بالسيتوبلازم، وتورماً متقطعاً في الميتوكوندريا وتغيرات نووية. في المقابل ، أظهرت المجموعة الفرعية التجريبية ٢C تغييرات تركيبية طفيفة و فرقا غير مهم في جميع المعلمات المذكورة.

الإستنتاج: غير البليوميسين التركيب الطبيعي للجلد في ذكور الجرذان البيضاء البالغة. حسنت الخلايا الجذعية الميزنشيمية المشتقة من نخاع العظم التغيرات الجلدية التي يسببها البليوميسين.